THE ASTRONOMICAL JOURNAL VOLUME 103, NUMBER 6 JUNE 1992

ASSOCIATION OF SUPERNOVAE WITH RECENT STAR FORMATION REGIONS IN LATE TYPE GALAXIES

SCHUYLER D. VAN DYK[1,2]

Naval Research Laboratory, Center for Advanced Space Sensing, Code 4215, Washington, DC 20375-5000

Received 6 December 1991; revised 11 February 1992

ABSTRACT

A statistical study has been carried out to constrain the various models for the progenitors of supernovae of types Ia, Ib/c, and II. Star formation regions in late type galaxies are traced out by H II regions, imaged through photographic and CCD observations, and possible supernova association with these regions is based on the ratio of the angular separation of each supernova from its nearest H II region to the angular extent of the H II region in the direction of the supernova. The specific problems of supernova classification and positional uncertainties, as well as the probability of chance superposition, are also considered. The results suggest that type Ia supernovae do not arise from massive, short-lived stellar populations. Type Ib/c and type II supernovae, however, are very likely to be associated with H II regions and therefore with massive stellar progenitors. The single Wolf–Rayet star progenitor model for the type Ib/c supernovae is not supported. It is not clear from the results whether a difference between the association of type Ib/c supernovae and the association of type II supernovae with H II regions exists, but this probably results from the effects of small-number statistics for the type Ib/c supernovae. Not all type Ib/c and type II supernovae were found to be associated with detected H II regions; these supernovae either may have had runaway O star progenitors or were associated with H II regions below detectability.

1. INTRODUCTION

Supernovae (SNe) are generally classified into three different categories, type Ia (hereafter referred to as SNe Ia), type Ib/c (hereafter referred to as SNe Ib/c; in this paper SNe Ib/c as a class will include both of the possible and very similar subtypes type Ib and type Ic), and type II (hereafter referred to as SNe II). Although the model fits to spectroscopic and photometric observations of SNe are often quite good (cf. Woosley & Weaver 1986 for a discussion of the overall physics involved in these models), it is still not exactly known which stellar populations give rise to these three different types of SNe, or whether, in fact, these populations are indeed different.

SNe II have been found to occur only in spiral and irregular galaxies, so it has long been assumed that these events are due to the explosions of single, massive, short-lived stars. SNe Ib/c exclusively occur in late type galaxies, which, along with the spectral evidence for a large oxygen yield (e.g., Filippenko & Sargent 1985; Gaskell *et al.* 1986; Begelman & Sarazin 1986) and the presence of He I in early-time spectra of type Ib SNe (e.g., Harkness *et al.* 1988; Wheeler & Harkness 1990), have led to speculation that these SNe may have massive progenitors, possibly Wolf–Rayet descendants of single stars with $\mathcal{M} \gtrsim 30\ \mathcal{M}_\odot$ (e.g., Ensman & Woosley 1988; Fransson & Chevalier 1989; Swartz & Wheeler 1991). Various observational and theoretical considerations, however, have cast doubt on a very high-mass single-star progenitor model for SNe Ib/c (e.g., Nomoto 1986; Branch & Nomoto 1986; Uomoto 1986; Weiler *et al.* 1986; Panagia & Laidler 1989; Wheeler & Harkness 1990; Nomoto *et al.* 1990; Hachisu *et al.* 1991) and argue instead for progenitors with masses ranging from 3 to 8 $\mathcal{M}_\odot$ within interacting binary systems.

SNe Ia occur in *all* galaxy types, leading to the prevailing wisdom that the progenitor population is old and evolved, possibly involving one or more white dwarfs in an interacting binary system. However, the preponderance of SNe Ia in late type galaxies, in which star formation is currently taking place, has led to the suggestion that SNe Ia may not be strictly due to a very old population, but may, in fact, also be the endpoints of a short-lived ($\lesssim 10^8$ yr) group of stars (Oemler & Tinsley 1979). Other observational evidence has been used to also suggest that SNe Ia progenitors in late type galaxies may be an intermediate-age population (Filippenko 1989) or groups of stars with a range of ages (van den Bergh 1990b). Such a dichotomy or range in possible progenitors would present an interesting paradox, considering growing evidence that SNe Ia are quite photometrically homogeneous, despite apparent spectroscopic differences (Leibundgut & Tammann 1990; Tammann & Leibundgut 1990; Leibundgut 1991).

One means of better constraining these various models is to explicitly consider the local galactic environments and likely stellar progenitors in these environments where SNe have occurred, rather than merely considering the global properties of the parent galaxies. This can be accomplished

[1]Naval Research Laboratory/National Research Council Cooperative Research Associate.

[2]Visiting Astronomer, Kitt Peak National Observatory, National Optical Astronomy Observatories, which are operated by the Association of Universities for Research in Astronomy, Inc., under contract with the National Science Foundation.

 0004-6256/92/061788-16$00.90

by selecting an identifiable component of the environment and considering the association of SNe with that component, with adequately large samples of SNe of the three types. Such a test can best be applied to late type (particularly Sc) galaxies, since these galaxies are most frequently parents of SNe of *all* types (Tammann 1982; Cappellaro & Turatto 1988; Evans *et al.* 1989; van den Bergh & Tammann 1991). The results of such a study can then be combined with the theoretical models in order to better understand the nature of SNe progenitor populations.

The environmental component chosen for these late type galaxies is H II regions, which are detectable through Hα emission arising from the ionizing flux of Lyman continuum photons emitted by hot massive young stars. These regions therefore serve as excellent indicators of the position and extent of recent ($\lesssim 10^7$ yr) massive star formation in the SNe parent galaxies and therefore serve as indicators of the relation between the three SN types and young, massive stellar progenitors.

Many of the H II regions in late type gas-rich parent galaxies are giant, with dimensions of hundreds of parsecs and luminosities $L_{H\alpha} \gtrsim 5\text{–}10 \times 10^{38}$ ergs s^{-1} (Kennicutt *et al.* 1989). Kennicutt (1991) reviews the overall properties of these giant regions. Although star formation, particularly massive star formation, is not restricted to these regions in late type galaxies (faint diffuse emission, due at least partly to unresolved clumps of smaller H II regions, is visible between the larger regions in many galaxies; e.g., Tully 1974; Courtes 1977), star formation is much more pronounced in the giant emission regions, and the number of massive stars responsible for the ionization must be large. Kennicutt *et al.* (1989) found that in late type spirals and irregulars the giant H II regions are sites of the majority of the massive star formation within these galaxies. Therefore SNe associated with these recent star-formation regions possess a greater chance of having had massive stars as progenitors than SNe which occurred well outside these H II regions.

Several previous studies (Richter & Rosa 1984; Huang 1987; Panagia & Laidler 1989) have considered the association of SNe with H II regions, but are much more restricted in scope than the present study. Panagia & Laidler restricted themselves to SNe Ib/c, Huang included SNe of all types but, unfortunately, did not segregate SNe Ia from SNe Ib/c, and Richter & Rosa only considered SNe in M101 and M83. Additionally, it is inadequate to base conclusions of the association of SNe with H II regions on assessments made by eye, as these previous studies have done, since judgments made about the dimensions of H II regions are subject to a number of intrinsic, instrumental, and perceptual effects (Kennicutt 1978). Furthermore, Huang did not consider the consequences of including in his sample SNe with uncertain classification, and neither Huang nor Panagia & Laidler considered uncertainties in SNe positions, which together are the primary sources of error in a study of this kind and can greatly influence its conclusions. Finally, none of the studies adequately considered the probability of chance superposition of SNe onto H II regions.

In this paper, the association of SNe with H II regions is made by comparing the projected angular separation of each SN from its nearest H II region with the angular radial extent of the H II region in the direction of the SN. If the proportion of apparent associations of SNe of a given type is appreciably larger than the probability of chance superposition, then those associations are likely to be real and that SN type is likely to arise from a massive stellar population. If the proportion of apparent associations does not exceed the probability of chance superposition, then the likelihood of association of SNe of a given type with a massive stellar population is small.

2. THE PROCEDURE

2.1 The SN Sample and H II Region Data

The sample of SNe considered in this paper was drawn from the Asiago Catalog of SNe (Barbon *et al.* 1989), which is complete through the end of 1988, and from the various IAU Circulars reporting the occurrences of SNe since that time to mid-1990. The sample was restricted to SNe which have been classified into types. Parent galaxies which are nearer to being face-on were generally favored over those which are seen at or near edge-on, in order to minimize any effects that galaxy inclination might have on the measurements of H II region dimensions and of the separations between H II regions and SNe. The average inclination for all galaxies in the sample is $\sim 45°$ (inclinations taken from Tully 1988). It is not yet clear what effect inclination might have on SNe rates and, therefore, how selecting parent galaxies more nearly face-on might influence the SNe included in our sample; van den Bergh (1990a) and van den Bergh & McClure (1990) found that the number of SNe apparently rises sharply for face-on galaxies with inclinations $\lesssim 30°$, with the numbers of SNe II and, possibly, of SNe Ib/c being affected more than the numbers of SNe Ia (van den Bergh & Tammann 1991), although this dependency of SNe rates on inclination was not found by Muller *et al.* (1992).

Our SN sample was first compared with a list (Hodge 1982) of galaxies for which catalogues of H II regions and corresponding maps are available from the literature. The various catalogues employed (Hodge 1966; Hodge 1969; Hodge 1974; Boeshaar & Hodge 1977; Hodge & Kennicutt 1983) provide accurate nuclear offset positions of the identified H II regions, so that the apparent locations of SNe relative to nearby H II regions could be easily located. Note that for all the above catalogues the regions were visually identified by the author on photographic plates (i.e., no isophotal or photometric criteria were used).

In order to measure the dimensions of the H II regions nearest the SNe in the sample, original Hα photographic plates were made available to us by Kennicutt (1986). The procedure for taking the plates is described in detail by Kennicutt (1978) and will not be recounted here. The H II region data were then augmented by obtaining CCD Hα images of several previously unmapped galaxies, either

TABLE 1. Type I supernovae.

SN (1)	SN type (Barbon *et al.* 1989) (2)	SN type (Branch 1986) (3)	Galaxy (4)	Galaxy type (5)
1937C	Ia	Ia	IC 4182	Sm
1954A	Ib/c[a]	Ipec	NGC 4214	SBmIII
1954B	I	I*	NGC 5668	ScII-III
1956A	I	I*	NGC 3992	SBbI[b]
1960F	Ia	Ia	NGC 4496a	SBcIII-IV
1960H	Ia	I*	NGC 4096	ScII-III
1962L	Ib/c	Ib	NGC 1073	SBcII
1963P	Ia	Ia	NGC 1084	ScII.2
1964L	Ib/c	Ib	NGC 3938	ScI
1966J	Ib/c	I*	NGC 3198	ScI-II
1967C	Ia	Ia	NGC 3389	ScII.2
1969C	Ia	Ia	NGC 3811	SBc
1971I	Ia	Ia	NGC 5055	SbcII-III
1971L	Ia	Ia	NGC 6384	SbI[c]
1974G	Ia	Ia	NGC 4414	ScII.2
1976D	Ia	–	NGC 5427	SbcI
1981B	Ia	Ia	NGC 4536	SbcI-II
1983I	Ib/c	–	NGC 4051	SbcII
1985F	Ib/c	–	NGC 4618	SBbcII.2pec
1987M	Ib/c	–	NGC 2715	ScII
1988L	Ib/c	–	NGC 5480	Sc
1990B	Ib/c	–	NGC 4568	ScII-III

[a]Barbon *et al.* (1989) refer to these SNe as Type Ib. Since many of these SNe were of the possible subtype Ic, we refer to this SN classification as Ib/c.
[b]NGC 3992 is listed as SBbc by Barbon *et al.* (1989).
[c]NGC 6384 is listed as Sbc by Barbon *et al.* (1989).

from other investigators or through observations made by us during three observing runs (in 1986 May, 1987 April, and 1989 May) using the KPNO 0.9 m telescope with the direct camera at focal ratio $f/7.5$ and during one run (in 1991 April) using the Lowell Observatory (hereafter referred to as LO) 1.1 m telescope with the direct camera at focal ratio $f/8$. The galaxies we observed were restricted to $m \lesssim 13$ (either B or photographic magnitude) and declination $\delta \gtrsim -20°$. To improve on the astrometry and photometry possible using the photographic plate data, much of this data were superceded by CCD data.

Table 1 lists the total sample of SNe Ia and SNe Ib/c and Table 2 lists the total sample of SNe II. In both tables the parent galaxy designation and classification, according to Sandage & Tammann (1981), are given in columns (4) and (5), respectively. In the few cases where no galaxy type was available in Sandage & Tammann, classification was derived from de Vaucouleurs *et al.* (1976). The galaxy types given in Tables 1 and 2 were checked against those given in Barbon *et al.* (1989), who used Sandage & Tammann and de Vaucouleurs *et al.* as their main sources for galaxy classification, and, as expected, general agreement exists, except in the cases of NGC 3992, NGC 5033, NGC 6384, and NGC 7331, where Barbon *et al.* list a later galaxy type (i.e., Sbc or Sc) than does Sandage & Tammann. Taking into account inevitable uncertainties in galaxy classification, it is nonetheless clear that we are considering galaxies of type Sbc or later.

The sources for the H II region data used in our study are listed in Table 3. Column (1) lists the parent galaxies for which H II region data was available; column (2) lists the UT observing epochs, if the observations were made by us; column (3) lists the observatories and detectors (i.e., plates or CCDs) used to acquire the H II region data; column (4) lists the filters (designated by their effective central wavelengths λ_{cent} in Å) used in our observations; column (5) lists the total exposure times (in s) for our observations; and, column (6) lists an estimate of the seeing (FWHM) for each set of our galaxy observations.

An attempt was made to keep the procedure for our CCD observations consistent with those used for the photographic plate observations (cf. Kennicutt 1978). Images on all three KPNO runs were made through narrow "on-band" and "off-band" interference filters, although the on-band Hα filters had larger bandwidths ($\sim$75 Å) than the bandwidths ($\sim$20 Å) used for the photographic dataset (Kennicutt 1978). The on-band Hα filters had either a central wavelength of 6563 or 6608 Å, to accommodate the range of systemic velocities of the observed galaxies. The off-band filter was centered in a line-free spectral region at $\sim$5125 Å, similar to the filter used for much of the photographic data, but with a bandwidth ($\sim$30 Å) somewhat narrower than the "special" filter described by Kennicutt (1978). For the LO run, the on-band Hα filters had central wavelengths either of 6570 or 6595 Å, depending on the observed galaxy's systemic velocity. The off-band (continuum) filter had a central wavelength of 6683 Å. The on-band filters were all substantially narrower than those used at KPNO, with bandwidths of $\sim$35 Å. The off-band filter had a comparable bandwidth to the off-band filter used at KPNO. For all runs, a series of short exposures (usually

TABLE 2. Type II supernovae.

SN (1)	SN type (Barbon *et al.* 1989) (2)	SN light curve subtype[a] (3)	Galaxy (4)	Galaxy type (5)
1917A	II	–	NGC 6946	ScII
1921B	II:	–	NGC 3184	ScII.2
1926A	II	P	NGC 4303	ScI.2
1936A	II	P	NGC 4273	SBcII
1937F[b]	II	P	NGC 3184	ScII.2
1941A	II	L	NGC 4559	ScII
1941C	II	–	NGC 4136	ScI-II
1948B	II	P	NGC 6946	ScII
1959D	II	L	NGC 7331	SbI-II[c]
1961F	IIpec	–	NGC 3003	ScII
1961I	IIpec	–	NGC 4303	ScI.2
1961U	II	L	NGC 3938	ScI
1964A	IIpec	–	NGC 3631	ScI-II
1964F	II	–	NGC 4303	ScI.2
1965H	II	–	NGC 4666	SbcII.3
1965L[b]	II	P	NGC 3631	ScI-II
1966B	II	L	NGC 4688	SBcII
1967H	II:	–	NGC 4254	ScI.3
1968D	II	–	NGC 6946	ScII
1970G	II	L	NGC 5457	ScI
1972Q[b]	II	P	NGC 4254	ScI.3
1975T[b]	II	P	NGC 3756	ScI-II
1978H	II	–	NGC 3780	ScII.3
1979C	II	L	NGC 4321	ScI
1980K	II	L	NGC 6946	ScII
1985H	II	–	NGC 3359	SBcI.8
1985L	II	–	NGC 5033	SbI[d]
1986I	II	–	NGC 4254	ScI.3
1987K	IIb	–	NGC 4651	ScI-II

[a]Light curve subtypes from Barbon *et al.* (1979).
[b]These SNe were classified as type II based on photometry alone. Although basing classifications on photometry is prone to errors, and although the reality of the SN II light curve subtypes, II-L and II-P, is debatable, we confirm the likelihood of these SNe being SNe II based on luminosity arguments as well (see Sec. 2.3).
[c]NGC 7331 is listed as Sbc by Barbon *et al.* (1989).
[d]NGC 5033 is listed as Sc by Barbon *et al.* (1989).

600 s in duration) were made of the program galaxies through both the on-band and off-band filters, and these short exposures were then co-added to produce one long-exposure image, with total exposure times given in column (5) of Table 3.

During the observing runs *B*- and *R*-band images (each with 600 s exposure times) were also obtained for most of the parent galaxies. These were used to assist in H II region and stellar association identification, location of the galactic nuclei, estimates of seeing, and measurement of the dimensions of the galactic disks. For all runs, a series of "dome flat" frames through all filters and "bias" frames were made and used in the image reduction. The preliminary reduction and processing of the CCD frames were made at KPNO using the observatory's standard reduction software and at LO using IRAF.

2.2 Photometric Calibration of the H II Region Data

Since surface-brightness limits are of interest for determination of H II region detectability and of the isophotal boundaries of H II region surface brightness profiles, the data had to be photometrically calibrated.

Calibration of the microdensitometry (see Sec. *2.5*) of photographic plate data for the H II regions of interest in NGC 1073, NGC 1084, NGC 3389, NGC 5055, and NGC 6384 was performed using the surface-brightness profile derived from the plate image of the giant H II region NGC 5472 in M101 (Kennicutt 1978; Hodge 1986) and using the profiles of H II regions derived from plate and CCD images of NGC 4254. This procedure is, of course, crude, and we naturally expect large errors in the photometry by using surface-brightness profiles extracted from one set of plates to calibrate another set of plates.

Calibration of the CCD images was performed using observations of several spectrophotometric standard stars. The standards were early G dwarfs, chosen for their lack of photometric variability, the availability of published continuum scanner data in the appropriate spectral regions, and accurate knowledge of the equivalent width of the Hα absorption line in the bandpasses of the filters (cf. Kennicutt 1978). The stars used (BD+26° 3780, HD 154760, HD 66171, HD 190605, HD 237822, BD+58° 1199, and HD 150205) were from the spectrophotometric atlases of Jacoby *et al.* (1984) and Gunn & Stryker (1983). Spectra

TABLE 3. Sources of H II region data.

Galaxy (1)	Observation date (UT) (2)	Observatory/ Detector (3)	Filter [λ_{cent} (Å)] (4)	Exposure time (s) (5)	Seeing (") (6)
NGC 1073	–	KPNO/Plate[a]	–	–	–
NGC 1084	–	KPNO/Plate	–	–	–
NGC 2715	1989 May 27	KPNO/RCA3[b]	5125	1800	2.1
			6608	1800	
NGC 3003	1989 May 28	KPNO/RCA3	5125	1800	2.6
			6608	1800	
NGC 3044	1989 May 29	KPNO/RCA3	5125	1200	2.6
			6608	1200	
NGC 3184	1991 April 09	LO/NSF TI[c]	6570	1800	3.0
NGC 3198	1986 May 20	KPNO/TI2[d]	5125	2000	2.2
			6563	4000	
NGC 3359	1989 May 30	KPNO/RCA3	5125	1800	2.9
			6608	1800	
NGC 3389	–	KPNO/Plate	–	–	–
NGC 3631	1989 May 31	KPNO/RCA3	5125	1200	2.2
			6608	1200	
NGC 3756	1989 May 27	KPNO/RCA3	5125	1800	1.6
			6608	1800	
NGC 3780	1989 May 31	KPNO/RCA3	5125	1200	2.3
			6608	1200	
NGC 3811	1987 April 20	KPNO/RCA3	5125	1200	3.0
			6608	1200	
NGC 3938	1989 May 29	KPNO/RCA3	5125	1800	2.7
			6563	1800	
NGC 3992	1986 May 18	KPNO/TI2	5125	1200	3.6
			6608	1800	
NGC 4051	1987 April 18	KPNO/RCA3	5125	1200	4.2
			6563	2400	
NGC 4096	1987 April 21	KPNO/RCA3	5125	1800	2.0
			6563	1800	
NGC 4136	1989 May 30	KPNO/RCA3	5125	1800	2.8
			6563	1800	
NGC 4214	1991 April 08	LO/NSF TI	6570	1200	3.4
NGC 4273	1989 May 28	KPNO/RCA3	5125	1800	3.2
			6608	1800	
NGC 4303	1991 April 09	LO/NSF TI	6595	1200	3.7
	–	KPNO/TI2[e]	–	–	–
NGC 4321	1989 May 30	KPNO/RCA3	5125	1200	2.5
			6608	1200	
NGC 4414	1987 April 20	KPNO/RCA3	5125	1200	3.3
			6563	1200	
NGC 4496a	1987 April 22	KPNO/RCA3	5125	1800	3.2
			6608	1800	
NGC 4536	–	KPNO/TEK 1[f]	–	–	–
NGC 4559	1991 April 09	LO/NSF TI	6570	1800	3.5
			6693	1800	
NGC 4568	–	KPNO/TEK 1	–	–	–
NGC 4618	1991 April 09	LO/NSF TI	6570	1200	3.1
			6693	1200	
NGC 4651	1989 May 30	KPNO/RCA3	5125	600	3.1
			6563	1200	
NGC 4666	1989 May 31	KPNO/RCA3	5125	1200	2.1
			6608	1200	
NGC 4688	1989 May 28	KPNO/RCA3	5125	600	3.8
			6563	600	
IC 4182	1987 April 20	KPNO/RCA3	5125	600	2.5
			6563	1200	
NGC 5033	1989 May 28	KPNO/RCA3	5125	1200	3.3
			6563	1200	
NGC 5055	–	KPNO/Plate	–	–	–
NGC 5427	–	KPNO/VCam[g]	–	–	–
NGC 5457	1989 May 27	KPNO/RCA3	5125	1200	2.4
			6563	600	

TABLE 3. (continued)

Galaxy (1)	Observation date (UT) (2)	Observatory/ Detector (3)	Filter [λ_{cent} (Å)] (4)	Exposure time (s) (5)	Seeing (″) (6)
NGC 5480	1991 April 09	LO/NSF TI	6595	1800	2.4
			6693	1800	
NGC 5668	1987 April 22	KPNO/RCA3	5125	1800	4.5
			6608	1800	
NGC 6384	–	KPNO/Plate	–	–	–
NGC 6946	1989 May 28	KPNO/RCA3	5125	600	3.2
			6563	1200	
	1989 May 29		5125	1800	2.5
			6563	1800	
NGC 7331	–	KPNO/VCam[h]	–	–	–

[a]The plate data are from Kennicutt (1986) and were taken using either the 0.9 or 2.1 m telescope at the Kitt Peak National Observatory (KPNO) through Hα filters of 20 Å bandwidth with central wavelengths appropriate for the systemic velocities of the galaxies (cf. Kennicutt 1978).
[b]The images were made using the RCA3 CCD on the KPNO 0.9 m telescope.
[c]The images were made using the NSF TI CCD on the Lowell Observatory (LO) 1.1 m telescope. This TI chip was not "preflashed" before every exposure.
[d]The images were made using the TI2 CCD, binned by two, on the KPNO 0.9 m telescope. The chip was "preflashed" for 10 s before every exposure to add an electron base to the bias level.
[e]Keel (1989) provided a continuum-subtracted image of NGC 4303 (including the sites of SNe 1926A and 1964F) made using the TI2 CCD on the KPNO 2.1 m telescope.
[f]Kenney (1990) provided continuum-subtracted flux-calibrated images of NGC 4536 and NGC 4568 made using the TEK 1 CCD on the KPNO 0.9 m telescope.
[g]Kennicutt (1986) provided a continuum-subtracted flux-calibrated image of NGC 5427 made using the Video Camera on the KPNO 2.1 m telescope.
[h]Keel (1989) provided a continuum-subtracted image of NGC 7331 made using the Video Camera on the KPNO 2.1 m telescope.

from Jacoby *et al.* had better signal to noise and resolution than spectra from Gunn & Stryker.

Standard star observations were used to determine the extinction coefficients for each night. The stars were observed in very short exposures through an appropriate range of airmasses. For three nights during the KPNO runs, either the coefficients could not be adequately determined from the observed standards due to nonphotometric conditions or not enough standards were observed for an accurate extinction relation to be computed. In these cases, average extinction coefficients at the central wavelengths of the filters were interpolated from the table of coefficients in the KPNO IRS spectrometer operating manual. Only the last night of the LO run was photometric. The extinction coefficients for observations through the on-band filters during the LO run were quite similar to the coefficients for observations through the on-band filters during the KPNO runs. The range of coefficients at 6563 Å for all runs was also similar to that found by Kennicutt (1978).

After the preliminary processing, all image processing of the galaxy and standard star images was done using AIPS. For each program galaxy the narrowband and broadband continuum images were aligned with the on-band image using foreground stars in common on all such images. The narrow off-band and on-band images of each galaxy were then appropriately flux calibrated using the standard star fluxes. The flux in the off-band image was scaled to the flux in the on-band image and was subtracted away, producing a continuum-subtracted Hα+[N II] image of the galaxy. For the KPNO runs, the continuum fluxes of the standard stars through the on-band filters were, on average, ~37% larger than the continuum fluxes through the off-band filter, so this nonzero slope of the continuum between filters necessitated a ~6% correction to the off-band flux subtracted away from the on-band flux for those galaxies. No such continuum flux correction was necessary for the galaxy images made during the LO run, since the on-band and off-band filters were essentially contiguous in wavelength.

A correction, although relatively small, was applied to the fluxes of galaxies observed both at KPNO and at LO which accounted for Hα absorption in the spectra of the calibration standards. Since the standard stars were all early G dwarfs, Hα equivalent widths were assumed to be equivalent to that for the Sun, i.e., ~4 Å (Moore *et al.* 1966). The corrections ranged from ~1% to ~11%, depending on the central wavelength and the bandwidth of the Hα filter.

Most radiation from H II regions is concentrated in emission lines, so it was necessary to assume that the Hα emission line profile is Gaussian throughout the flux calibration of all on-band galaxy images. The profile peak was defined at the central wavelength of the Hα line in each galaxy's reference frame at rest (systemic velocities were either from Sandage & Tammann 1981 or Palumbo *et al.* 1983). Deviations of the individual H II region velocities within a galaxy from the systemic velocity were assumed to be small. The dispersion in the Hα line was assumed to be 1.4 Å (FWHM), after Arsenault & Roy (1986), who found an average (Gaussian) velocity dispersion of ~27 km s^{-1} (0.6 Å at Hα) within the H II regions they studied.

Since the Hα filters used for both the photographic and CCD data were wide enough to include the [N II] satellite doublet, the amount of contamination by these lines to the net line flux was determined and eliminated. Since no spectrophotometry has been done for the H II regions of interest in these galaxies, a representative value of the contamination, ~30%, was assumed (e.g., Piembert & Torres-

Piembert 1974, 1976; Dufour 1975; de Goioa-Eastwood *et al.* 1984).

Finally, the extinction across and internal to many of these H II regions in the galaxies could be appreciable, with giant H II regions typically suffering 1–2 mag of extinction at Hα (Kennicutt 1988). The extinction internal to H II regions can also be radially variable (Koornneef 1978; Viallefond & Goss 1986), and can include large amounts of internal dust (Viallefond & Goss 1986). Since optical or radio spectral observations have generally not been made for the H II regions of interest, at best the fluxes can only be corrected for estimates of the Galactic extinction toward each galaxy (from Burstein & Heiles 1984) and for the internal extinction within the galaxy (from Sandage & Tammann 1981). The total extinction in the B band, A_B, was converted to the total extinction at Hα, $A_{H\alpha}$, using an extinction curve

$$A_B/A_V=1.29, \quad (1)$$

and the relation

$$A_{H\alpha}=0.81A_V, \quad (2)$$

from Viallefond & Goss (1986).

We can check the accuracy of our CCD image calibration through a comparison of our photometry of some of the brightest H II regions in NGC 3938, NGC 4254, and NGC 4321 with similar photometry by Kennicutt (1988). The photometry here was done using synthetic apertures in AIPS similar in size to those used by Kennicutt. Agreement between our photometry and that by Kennicutt appears good to $\sim$14% (ranging from 8% to 28%), although Kennicutt only corrected for Galactic extinction, and differences may also exist in filter transmission, corrections for [N II] contamination, etc. It is estimated, then, that photometry from our CCD observations as a whole is generally accurate to $\sim$10%–20%.

The images of NGC 4303 and NGC 7331 by Keel (1989) and the image of NGC 4303 obtained by us on a nonphotometric night at LO were calibrated using the Hα nuclear aperture photometry by Keel (1983) and Keel *et al.* (1985). All photometry for these galaxies had to be corrected for [N II] contamination as well as for internal galactic extinction. The images of NGC 4536 and NGC 4568 by Kenney (1990) had already been flux calibrated, but they required corrections for extinction and [N II] contamination. We obtained only an on-band image for NGC 3184 at LO, but the image, although not continuum subtracted, was calibrated using aperture photometry of H II regions by Kennicutt (1988); the amount of continuum contributing to the overall flux from the H II region of interest in this galaxy is small, so it was possible to find an adequate limiting surface brightness for the measured H II region profile.

2.3 SNe Types and Their Uncertainties

The types for the SNe in our sample are adopted from Barbon *et al.* (1989) and are given in column (2) of Tables 1 and 2. (The SN type for SN 1990B given in Table 1 is from Filippenko 1990 and Kirshner & Leibundgut 1990.) In addition, the SNe I types from Branch (1986) are given in column (3) of Table 1, and the SNe II light curve subtypes, "plateau" type (hereafter referred to as SNe II-P) and "linear" type (hereafter referred to as SNe II-L), from Barbon *et al.* (1979) are given in column (3) of Table 2.

Although Barbon *et al.* (1989) refer to SN type Ib, we refer to this classification as type Ib/c. The SNe Ib/c may possibly consist of two subtypes, type Ib, which show strong He I lines in their early time spectra, and type Ic, which show weak He I lines (see, e.g., Wheeler & Harkness 1990). However, it is not clear whether sufficient observational differences exist, especially in their late-time spectra, to justify two subtypes (Filippenko & Shields 1990; Filippenko 1991b). Also, it appears that almost all SNe Ib/c are actually type Ic (Filippenko 1991b). Furthermore, some models for the two subtypes involve the same physics and are based on very similar ranges of progenitor masses (e.g., Nomoto *et al.* 1990; Hachisu *et al.* 1991; Shigeyama *et al.* 1990). Therefore, we do not make a formal distinction between type Ib and type Ic SNe.

Additionally, no distinctions are made for the possible "type IIb" SNe, with narrow interstellar lines, discussed by Schlegel (1990), or "transforming" SNe, such as SN 1987K, discussed by Filippenko (1988b, 1991b). They are included with the SNe II. The SNe types III, IV, and V (Zwicky 1965) are considered as peculiar SNe II by Doggett & Branch (1985), and the few examples in our sample are also included with the "normal" SNe II. Finally, no formal distinction is made between the SNe II-P and SNe II-L (Barbon *et al.* 1979), although a brief discussion regarding possible differences in progenitors will be offered below.

Misidentification of SN type can greatly perturb the conclusions made in a study of this kind. Classification solely based on photometry may result in misclassification, since SNe light curves often suffer from uncertainties in shape measurement (including similarities between some SNe I and SNe II light curves) and from incomplete temporal coverage (see Harkness & Wheeler 1990 and Kirshner 1990 for discussions of classification and light curves). Classification by means of spectroscopy is therefore favored over classification made on the basis of photometry. The presence of broad H emission lines in the spectra of SNe II near maximum light, and their absence in SNe I, define these two general SNe groups. Similarly, the presence or absence of the λ6150 feature in the spectra of SNe Ia and Ib/c, respectively, clearly distinguishes these SN types. Huang's (1987) study of the association of SNe with H II regions may have been affected by the inclusion of SNe classified by their light curves or poor quality spectra.

Unfortunately, although Barbon *et al.* (1989) indicate that their SNe types are derived mostly from spectroscopy, they do not provide any explicit indications which SNe were classified based on spectroscopy or photometry. We determined the basis for the classifications of the SNe in Tables 1 and 2 by examining the original literature, using Flin *et al.* (1979) as a reference guide for SNe occurring before 1976. All of the SNe Ia in Table 1 were classified

based on spectroscopy. SNe Ib/c are always strictly classified in spectroscopic terms.

Two of the SNe in Table 1, SN 1954B and SN 1956A, were classified as type I by Barbon *et al.* (1989); Branch (1986) classified these SNe as "type I*," indicating that their spectra are consistent with being either of type Ia or Ib/c. We assume in our statistics that SNe 1954B and 1956A were likely to be SNe Ia, rather than SNe Ib/c, since their maximum B-band absolute magnitudes, $M_B(\max)$, were ~ -19.4 and ~ -18.4, respectively (calculated from the maximum apparent magnitudes given for these SNe in Barbon *et al.* 1989, and assuming $H_0 = 75$ km s^{-1} Mpc^{-1} and $m_B \simeq m_{pg} + 0.3$), which are more similar to the assumed absolute magnitude for SNe Ia, $M_B(\max) \simeq -18.9$, from van den Bergh & Tammann (1991), than to the assumed absolute magnitude for SNe Ib/c, $M_B(\max) \simeq -17.3$.

Most of the SNe II in Table 2 were classified based on spectroscopy. Four SNe, SN 1937F, SN 1965L, SN 1972Q, and SN 1975T, were classified as SNe II based on photometry alone, and were subtyped by Barbon *et al.* (1979) as SNe II-P. It is, of course, understandable that Barbon *et al.* (1989) would consider the light curve subclassification as sufficient evidence for these SNe being SNe II. We confirm, based on similar luminosity arguments to those above (the maximum absolute magnitudes of these SNe were $M_B[\max] \sim -15.7$, -16.7, -15.3, and -16.2, respectively, which is sufficiently similar to the assumed $M_B[\max] \simeq -16.3$ for SNe II from van den Bergh & Tammann 1991), that it is likely these were SNe II, and we assume that this is the case in our statistics.

For both the SNe Ia and SNe II, the presence in the statistics of those few SNe with uncertainties in their classifications might result in a negative effect on the conclusions reached in this paper regarding the association of SNe with H II regions. For lack of a better or more accurate discriminator to reduce what impact that these SNe might have, we will assign these SNe half the weight of the well-classified SNe in the sample when computing in Sec. *3.1* the proportions of SNe associated with H II regions, although we acknowledge that such a weighting scheme is not without its pitfalls.

Finally, we note that the majority of well-classified SNe in parent galaxies which meet our criteria for observation have actually been considered in our sample. Excluding galaxies with $\delta < -20°$ and $m \gtrsim 13$, the numbers of SNe which are listed in Barbon *et al.* (1989) as SNe Ia, SNe Ib/c, and SNe II, and which occurred in galaxies of type Sbc and later, are 20, 9, and 32, respectively. In our sample, 11 SNe Ia, 7 SNe Ib/c, and 25 SNe II from Barbon *et al.*, all with spectroscopic classifications, are considered, so that better than $\sim 55\%$ of all well-classified SNe in galaxies of interest comprise our sample.

2.4 SNe Nuclear Offset Positions and Their Uncertainties

Another factor which can affect the results of this study is the uncertainty in the positions of SNe within their parent galaxies. Unfortunately, it has historically been the practice to express the position of a SN relative to the parent galaxy nucleus, which itself is often imprecisely defined. Furthermore, several positions are often given in the literature for each SN, with generally no corresponding indication of the uncertainties in the measurements of these positions.

Barbon *et al.* (1989) provide "best estimate" offset positions for SNe, pointing out that "large discrepancies in [positional] data from different authors" may exist for SNe, but unfortunately they do not detail what criteria were used to assess the quality of the positions that comprised their estimates, making the use of their positional estimates somewhat questionable. Therefore, all available offset positions for each SN in the sample were obtained from the original literature, again using Flin *et al.* (1979) as a guide for all SNe occurring before about 1976, and various sources, primarily IAU Circulars, for SNe occurring since then. If more than one position existed for a SN, then an average position was derived from these several positions. If the position of a SN could not be located elsewhere in the literature, then the position given by Barbon *et al.* (1989) was used. The adopted SN nuclear offset positions are given in column (2) of Tables 4, 5, and 6.

Marsden (1982) states that the total uncertainty level in offset positions quoted in the IAU Circulars is of order $\pm 10''$. We found for those SNe with more than one position given in the literature that the scatter about the average position derived from the several positions was generally less than this error. On the other hand, we suspect for SNe observed in the early decades of this century, which typically have only one position available in the literature, that the positions may be in error by more than $10''$. We assume here that $10''$ is representative of the total uncertainty in the offset positions for those SNe for which no indication of precise uncertainties exist, whether the offset positions came from the IAU Circulars or not.

The quality and accuracy of the positions for several SNe which occurred during the last twenty years were assessed using information provided by Rupen (1991). Many of these SNe have total positional uncertainties at better than $1''$. Some have offset positions given in the literature expressed to tenths of an arcsec. We assume $1''$, which is well within the errors of this study, as the uncertainty in the positions of these recent SNe, although we realize that the actual positional uncertainties could be less than this. The assumed errors for each SN offset position are indicated in the notes to Tables 4, 5, and 6.

Similar to the assumed compensation in Sec. *2.3* for uncertainties in SNe types, we allow for the effects that (usually unknown) positional uncertainties might have on the results by assigning different weights to the SNe in the sample. Since the assumed SNe positional uncertainties are crude, again for lack of a better discriminator, we have simply given those SNe with an assumed uncertainty of $10''$ half the weight of those SNe with an assumed uncertainty of $1''$ when computing in Sec. *3.1* the proportions of SNe associated with H II regions.

TABLE 4. Measured quantities for H II regions nearest SNe Ia.

SN (1)	SN nuclear offset (″) (2)	H II region nuclear offset (″) (3)	r_{max}[a] (″) (4)	Δ[b] (″) (5)	R[c] (6)
1937C	30 E 40 N	1 E 21 N	4.7	34.6	7.4
1954B	15 W 23 S	2 E 15 S	8.2	18.8	2.3
1956A	67 E 9 S	83 E 3 S	5.4	18.4	3.4
1960F	43 E 26 N	28 E 17 N	8.3	17.5	2.1
1960H	67 E 114 N	25 E 45 N	–	80.1	–
1963P	33 E 8 S	25 E 4 S	6.0	11.5	1.9
1967C	43 W 44 N	36 W 17 N	5.9	10.2	1.7
1969C	5 E 4 N	nucleus	9.0	6.4	0.7
1971I	2 W 147 S	2 E 92 S	–	59.1	–
1971L	27 E 20 N	32 E 15 N	3.0	16.8	5.6
1974G	25 E 56 S	42 E 61 S	4.6	18.0	3.9
1976D	35 E 34 N	36 E 37 N	2.4	2.9	1.2
1981B	41 E 41 N	38 E 43 N	3.3	2.8	0.8

Notes to TABLE 4

[a]Defined as the maximum angular radius of a H II region measured in the direction of a SN.
[b]Defined as the angular separation between a SN position and a H II region centroid position.
[c]$R \equiv \Delta / r_{max}$. SN 1937C: SN offset from Barbon *et al.* (1989). Total error in offset ±10″. SN 1954B: SN offset is average of offset positions from Wild (1960) and Kowal *et al.* (1974). Total error in offset ±10″. SN 1956A: SN offset from Zwicky & Karpowicz (1965). Total error in offset ±10″. SN 1960F: SN offset is average of offset positions from Humason *et al.* (1961) and Bertola (1964). Total error in offset ±10″. SN 1960H: SN offset from Humason *et al.* (1961) and Barbon & Capaccioli (1976). Total error in offset ±10″. SN 1963P: SN offset from Zwicky (1964). Total error in offset ±10″. SN 1967C: SN offset from Barbon *et al.* (1989). Total error in offset ±10″. SN 1969C: SN offset is average of offset positions from Rosino (1969), Detre (1969), and Bertola & Ciatti (1971). Total error in offset ±10″. SN 1971I: SN offset from Dunlap (1971a) and Barbon *et al.* (1973b). Total error in offset ±10″. SN 1971L: SN offset from Dunlap (1971b). Total error in offset ±10″. SN 1974G: SN offset is average of offset positions from Schürer (1974), Patchett & Wood (1976), and Ciatti & Rosino (1977). Total error in offset ±10″. SN 1976D: SN offset from Searle (1976). Total error in offset ±10″. SN 1981B: SN offset from Barbon *et al.* (1989). Total error in offset ±1″.

It should also be noted that, for the photographic dataset, errors exist in the nuclear offset positions of the catalogued H II regions. Although only one set of coordinates is provided for each H II region in each galaxy, the errors in the positions of H II regions catalogued by, e.g., Hodge & Kennicutt (1983), amounted from various sources of error to a total of ~2″–4″. These errors do not substantially affect the results below, since most of the galaxies first considered from the plate dataset were reobserved using CCDs. On the CCD images the relative separations between the position of the galactic nucleus and the position of the H II region core were considered for each SN; therefore errors in H II region offset positions were not a factor.

2.5 *Measurement of H II Region Dimensions*

H II region dimensions were determined in this paper from isophotal measurements, rather than from subjective

TABLE 5. Measured quantities for H II regions nearest SNe Ib/c.

SN (1)	SN nuclear offset (″) (2)	H II region nuclear offset (″) (3)	r_{max}[a] (″) (4)	Δ[b] (″) (5)	R[c] (6)
1954A	84 E 216 S	43 E 162 S	–	67.5	–
1962L	10 E 77 N	1 W 85 N	4.8	13.6	2.8
1964L	3 W 31 N	6 W 33 N	4.7	3.6	0.8
1966J	100 W 165 S	87 W 126 S	2.0	40.3	20.2
1983I	22 E 52 S	23 E 52 S	5.0	1.0	0.2
1985F	11.9 E 4.9 N	10.1 E 3.4 N	8.3	2.3	0.3
1987M	4.5 E 17.0 N	0.6 E 18.2 N	2.1	4.1	2.0
1988L	3.3 E 14.3 N	15.5 E 8.1 N	7.8	13.7	1.8
1990B	6 W 10 N	5 W 9 N	6.2	1.0	0.2

Notes to TABLE 5

[a]Defined as the maximum angular radius of a H II region measured in the direction of a SN.
[b]Defined as the angular separation between a SN position and a H II region centroid position.
[c]$R \equiv \Delta / r_{max}$. SN 1954A: SN offset from Wild (1954). Total error in offset ±10″. SN 1962L: SN offset from Barbon *et al.* (1989). Total error in offset ±10″. SN 1964L: SN offset from Bertola *et al.* (1965). Total error in offset ±10″. SN 1966J: SN offset from Schürer (1966). Total error in offset ±10″. SN 1983I: SN offset from Tsvetkov (1985). Total error in offset ±10″. SN 1985F: SN offset derived from the absolute position of SN 1985F given by Filippenko & Sargent (1986) and from the absolute position of the bar center given by Odewahn (1991a). Additionally, the nearest H II region offset was derived from its absolute position (α[1950.0] = $12^h39^m09^s.44$, δ[1950.0]=41°25′31″.2) given by Odewahn (1991b). Total error in offset ±1″. SN 1987M: SN offset from Porter (1987). Total error in offset ±1″. SN 1988L: SN offset from Perlmutter & Pennypacker (1988). Total error in offset ±1″. SN 1990B: SN offset from Perlmutter & Pennypacker (1990). Total error in offset ±1″.

TABLE 6. Measured quantities for H II regions nearest SNe II.

SN (1)	SN nuclear offset (″) (2)	H II region nuclear offset (″) (3)	r_{max}[a] (″) (4)	Δ[b] (″) (5)	R[c] (6)
1917A	37 W 105 S	41 W 112 S	6.3	7.9	1.2
1921B	32 E 160 S	43 E 161 S	3.6	11.0	3.1
1926A	11 W 69 N	8 W 70 N	0.7	3.1	4.4
1936A	29 N	1 E 21 N	7.0	8.0	1.1
1937F	5 E 149 S	19 E 139 S	2.2	12.2	5.5
1941A	30 W 26 N	29 W 27 N	5.4	1.9	0.4
1941C	44 E 67 S	67 E 63 S	10.0	23.4	2.3
1948B	222 E 60 N	229 E 65 N	23.6	9.0	0.4
1959D	32 W 13 N	29 W 12 N	2.1	2.8	1.3
1961F	34 E 17 N	34 E 18 N	4.0	0.6	0.2
1961I	82 E 12 S	81 E 13 S	5.6	0.6	0.1
1961U	81 E 104 N	76 E 101 N	11.2	6.2	0.6
1964A	74 W 92 N	72 W 82 N	5.7	10.3	1.8
1964F	25 W 3 S	26 W 5 S	3.8	4.4	1.2
1965H	22 W 29 S	20 W 23 S	4.8	6.6	1.4
1965L	42 W 64 N	41 W 58 N	2.9	6.1	2.1
1966B	24 W 38 S	27 W 40 S	5.0	3.1	0.6
1967H	80 E 19 S	79 E 13 S	6.4	5.9	0.9
1968D	45 E 20 N	45 E 16 N	4.2	4.3	1.0
1970G	98 W 383 S	100 W 390 S	12.3	7.3	0.6
1972Q	16 E 95 N	11 E 94 N	3.6	5.3	1.5
1975T	54 W 34 S	14 W 43 S	4.6	40.9	8.9
1978H	14 E 13 S	15 E 13 S	2.9	0.9	0.3
1979C	52.9 E 87.8 S	54.0 E 87.5 S	1.5	1.1	0.7
1980K	283.6 E 165.2 S	225.3 E 148.6 S	–	60.6	–
1985H	34.8 W 21.6 N	34.3 W 22.0 N	4.1	0.7	0.2
1985L	70 W 55 N	61 W 55 N	5.0	8.5	1.7
1986I	36 E 16 S	36 E 15 S	2.2	1.5	0.7
1987K	22 W 5 N	18 E 5 N	5.3	4.0	0.8

Notes to TABLE 6

[a]Defined as the maximum angular radius of a H II region measured in the direction of a SN.

[b]Defined as the angular separation between a SN position and a H II region centroid position.

[c]$R \equiv \Delta / r_{max}$. SN 1917A: SN offset from Curtis (1917). Total error in offset ±10″. SN 1921B: SN offset from Shapley (1939) and Bertaud (1949). Total error in offset ±10″. SN 1926A: SN offset from Barbon *et al.* (1989). Total error in offset ±10″. SN 1936A: SN offset from Hubble & Moore (1936). Total error in offset ±10″. SN 1937F: SN offset from Shapley (1939). Total error in offset ±10″. SN 1941A: SN offset from Jones (1941a). Total error in offset ±10″. SN 1941C: SN offset from Jones (1941b). Total error in offset ±10″. SN 1948B: SN offset from Mayall (1948). Total error in offset ±10″. SN 1959D: SN offset from Zwicky (1965). Total error in offset ±10″. SN 1961F: SN offset from Wild (1961). Total error in offset ±10″. SN 1961I: SN offset from Zwicky (1965). Total error in offset ±10″. SN 1961U: SN offset from Bertola (1963) and Zwicky (1965). Total error in offset ±10″. SN 1964A: SN offset from Ciatti & Barbon (1971). Total error in offset ±10″. SN 1964F: SN offset from Rosino (1964). Total error in offset ±10″. SN 1965H: SN offset from Haro (1965). Total error in offset ±10″. SN 1965L: SN offset is average of offset positions from Löchel (1965) and Ciatti & Barbon (1971). Total error in offset ±10″. SN 1966B: SN offset from Gates *et al.* (1967). Total error in offset ±10″. SN 1967H: SN offset from Zwicky (1967, 1968). Total error in offset ±10″. SN 1968D: SN offset from Wild (1968). Total error in offset ±10″. SN 1970G: SN offset from Barbon *et al.* (1973a). Total error in offset ±10″. SN 1972Q: SN offset from Wild (1972). Total error in offset ±1″. SN 1975T: SN offset from Wild (1975). Total error in offset ±1″. SN 1978H: SN offset from Wild (1978). Total error in offset ±1″. SN 1979C: SN offset from radio positions of SN and galactic nucleus from Weiler *et al.* (1991). Total error in offset ±1″. SN 1980K: SN offset measured from Fig. 1 of Thompson (1982). Total error in offset ±1″. SN 1985H: SN offset from Wheeler (1985). Total error in offset ±1″. SN 1985L: SN offset from Sinclair (1985). Total error in offset ±1″. SN 1986I: SN offset from Pennypacker *et al.* (1986). Total error in offset ±1″. SN 1987K: SN offset from Pennypacker (1987) and Filippenko (1988b). Total error in offset ±1″.

eye-based measurements. For a full discussion of the advantages of using isophotally defined measurements, cf. Kennicutt (1978).

For the photographic data, the nearest H II region to each SN was identified by finding the smallest separation between the catalogued offset positions of H II regions in the SN's parent galaxy and the adopted SN position. In some cases, corresponding photographs of SNe taken during occurrence, when available from the literature, aided visual identification of the SN positions on the photographic plates.

The CCD galaxy images provided better signal-to-noise and continuum subtraction, so that fainter H II regions could potentially be identified than was true for the photographic data. H II regions on CCD images were generally more luminous than $\sim 5 \times 10^{37}$ ergs s^{-1} (at the Virgo cluster distance from Tully 1988; for our sample, with distances from Tully 1988, this limit ranged from $\sim 5 \times 10^{36}$ to $\sim 2 \times 10^{38}$ ergs s^{-1}). For these images the centroid of the galactic nucleus on a continuum (usually B) image was determined to define the positions of the SN and nearest H II region (the Hα emission region above the detection limit whose centroid had the smallest separation from the SN position) on the continuum-subtracted Hα

image. All centroids were determined using the routine *MAXFIT* in AIPS.

For the plate data, microdensitometry was done at the University of Washington. For each SN the nearest H II region centroid was located by finding the maximum plate density and radially tracing through the SN position. The angular scales of the tracings were established by measuring the separation between the centroids of two foreground stars seen on both the Palomar Observatory Sky Survey (POSS) prints and on Hα plates taken at the 0.9 and 2.1 m telescopes.

The microdensitometer tracings were transformed to surface-brightness profiles. The maximum angular radius (r_{max}) of each H II region in the direction of a SN was defined as the point where the H II region emission was no longer distinguishable from plate noise or faint interregion emission, depending on the specific environment of each region. This maximum extent was generally at $\sim 3 \times 10^{-16}$ ergs cm^{-2} s^{-1} arcsec^{-2}, which is consistent with the isophotal radius threshold set by Kennicutt (1988). Errors in r_{max} measured in this manner are estimated to be $\lesssim$1.″0–1.″5.

For the CCD data surface-brightness profiles were obtained within AIPS by slicing from the nearest H II region centroid through the SN position. Since the profiles obtained from the CCD images were continuum subtracted, the maximum angular radius r_{max} of each profile was defined as the point where the Hα emission was indistinguishable from image noise, generally at $\sim 2 \times 10^{-17}$ ergs cm^{-2} s^{-1} arcsec^{-2}. This is a factor of $\sim$15 fainter than for the photographic data, which implies that r_{max} measured for a H II region on a CCD image would be larger than that measured on a photographic plate. The only galaxies imaged on photographic plates which were not subsequently imaged using CCDs were NGC 1073, NGC 1084, NGC 3389, NGC 5055, and NGC 6384; it is possible that r_{max} for the H II regions nearest the SNe in these galaxies may be underestimated, which could have some effect on the results in Sec. *3.1*.

Most SNe were found to occur well within $\sim$40″ of a detected H II region. However, in three cases (SN 1954A in NGC 4214, SN 1971I in NGC 5055, and SN 1980K in NGC 6946; see Tables 4, 5, and 6), the SNe occurred $\gtrsim$40″ from any identifiable H II region. They therefore could not be related to any detectable nearby H II region.

None of the profiles were corrected for seeing effects, since such corrections are generally small (1″–2″; Kennicutt 1978) and are well within other errors, e.g., those in the SNe offset positions themselves.

The measurements of the maximum H II region radii, r_{max}, are listed in Table 4 for the SNe Ia, in Table 5 for the SNe Ib/c, and in Table 6 for the SNe II. The nuclear offset positions of the nearest H II regions, either catalogued or directly measured from CCD images, are given in column (3) of each table. If the SN position was expressed with a decimal point, the H II region position is expressed likewise (if such precision is available); otherwise, the H II region position is expressed to the nearest arcsec. The maximum angular radii r_{max} of the nearest H II regions are given in column (4) of each table. The quantity Δ is defined for each SN as the angular separation between the SN position and the H II region position and is given in column (5) of each table. For each SN the ratio of Δ to r_{max} is defined as R, which is given in column (6) of each table.

TABLE 7. Association of SNe with H II regions.

SN type (1)	Proportion of SNe with $R \leqslant 1.0$ (2)	$R \leqslant 2.0$ (3)	$R \leqslant 3.0$ (4)
Ia	0.23 (±0.09)	0.46 (±0.13)	0.58 (±0.15)
Ib/c	0.46 (±0.19)	0.77 (±0.24)	0.85 (±0.26)
II	0.54 (±0.09)	0.80 (±0.11)	0.84 (±0.11)

3. THE RESULTS

3.1 Proportions of SNe Associated With H II Regions

The association of a SN with a H II region is determined by the value of the ratio R defined in Sec. *2.6* to be $R \equiv \Delta / r_{max}$. Ideally, if $R \leqslant 1$, then a SN is considered associated with a H II region. However, since an indeterminable uncertainty in R exists for most SNe, arising primarily from unknown uncertainties in Δ (we only crudely account for these uncertainties through the weighting scheme in Sec. *2.4*), we compute the proportion of SNe of a given type (including the weighting scheme to compensate for SNe classification uncertainties discussed in Sec. *2.3*) for $R > 1$ as well, which further allows for the uncertainty in the actual positional errors for most SNe.

The resulting cumulative proportions of SNe associated with H II regions are presented in Table 7 and shown in Fig. 1 for $R \leqslant 1$, $R \leqslant 2$, and $R \leqslant 3$. Also given for the proportions of SNe are their statistical errors, $\sqrt{N_{assoc}}/N_{SNe}$, where N_{assoc} is the number of SNe of a given type associated with H II regions and N_{SNe} is the total number of SNe of that type.

One can see that the proportions of SNe Ia are quite different from those for SNe Ib/c and SNe II. Specifically, the proportions of SNe associated with H II regions are substantially larger for SNe Ib/c and SNe II than for SNe Ia, implying that SNe Ib/c and SNe II are far more frequently associated with H II regions than are SNe Ia.

Comparing the proportions for SNe Ib/c and for SNe II, it is not clear that any significant difference exists between them, implying that SNe Ib/c and SNe II are associated with H II regions with equal frequencies. This result therefore implies that SNe Ib/c and SNe II are associated with similar stellar populations. But we must be careful drawing firm conclusions here, since, with only nine SNe Ib/c considered in our sample, the proportions for the SNe Ib/c likely suffer from the effects of small-number statistics. It is imperative that the environments of additional SNe Ib/c be observed to improve their statistics and see whether this possible trend continues to hold. Unfortunately, the increase in the number of SNe Ib/c in a sample of this kind may only be incremental, since the number of

late type galaxies meeting our observing criteria which have yet to be mapped in Hα and which were parents to known SNe Ib/c is small.

One interesting aspect of the proportions of SNe Ib/c and SNe II is that not all of these SNe were found associated with detected H II regions, even out to three H II region radii. The possible implications of this result are discussed below.

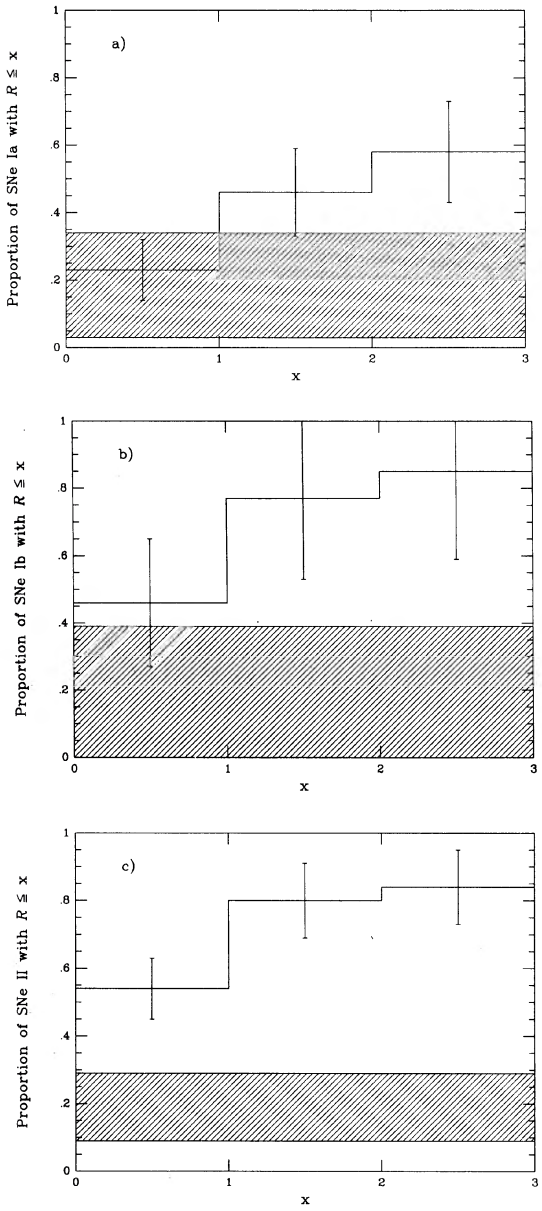

FIG. 1. (a) Distribution of the cumulative proportions of SNe Ia in our sample with $R \leqslant x$, where $x=1$, 2, and 3 and $R \equiv \Delta / r_{max}$, with Δ being the angular separation between a SN and the H II region nearest to it and r_{max} being the maximum angular radius of the H II region measured in the direction of the SN. The statistical errors in these proportions are shown as error bars. Also shown as the hatched band across the figure is the range in the probability of chance superposition. (b) Same as in (a), but for the SNe Ib/c. (c) Same as in (a), but for the SNe II. One can see that the proportions of SNe Ib/c and SNe II associated with H II regions are substantially larger than the proportion of SNe Ia. The proportions of SNe Ib/c and SNe II may not be significantly different from each other, but interpretation of this result may be hampered by the effects of small-number statistics for the SNe Ib/c.

We can discount that any differences which may exist between the three sets of proportions arise from distance effects. Although both r_{max} and Δ depend on parent galaxy distance, such that at large distances small, faint H II regions become more difficult to detect and small separations between SNe and H II regions become more difficult to measure, the ratio R is distance independent. Furthermore, the distributions as a function of systemic velocity for parent galaxies of all three SNe types are very similar and cover the same range of velocities. As mentioned above, galaxies with relatively low inclination were favored over those with high inclination, and the ranges in inclination were roughly the same for parent galaxies of SNe of each type, so differences between the three sets of proportions due to galactic inclination is minimal.

3.2 Probability of Chance Superposition

In order to determine whether the apparent SN-H II region associations found in Sec. *3.1* are likely to be physically real, we must estimate what the probability is that these associations for SNe of a given type would be expected by chance. The probability of chance superposition of SNe onto H II regions can simply be estimated as the fractional area of the parent galactic disks covered by detected H II regions, with the area of the galactic disks defined using continuum (usually B) images of the galaxies. For 20 galaxies with low inclination and with disks completely imaged on the CCDs, the average fractional area, and therefore the probability of chance superposition, is $\sim$0.19. However, we must account for the fact that neither the SNe nor the H II regions are randomly distributed across the galaxies. When the distributions of SNe are directly compared with the distributions of H II regions for these galaxies, we estimate that the probability of chance superposition ranges from 0.03 to 0.34 for SNe Ia, from $\sim$0 to 0.39 for SNe Ib/c, and from 0.09 to 0.29 for SNe II.

Comparing the ranges in these probabilities to the proportions of SNe apparently associated with H II regions given in Table 7 and shown in Fig. 1, we see that the proportion of SNe Ia with $R \leqslant 1$ is not significantly different from what would be expected by chance (even within the statistical errors, the proportion of SNe Ia with $R \leqslant 2$ does not exceed the probability of chance superposition), leading us to infer that these associations are not real and that the small proportion of SNe Ia found to be apparently associated with H II regions just represents chance superpositions of SNe onto those regions.

For the SNe Ib/c, although the proportion of SNe with $R \leqslant 1$ exceeds the range in the probability of chance superposition, if we consider the statistical errors, we cannot be entirely certain whether this proportion significantly exceeds what would be expected by chance. This lack of certainty is undoubtedly due to the effects of small-number

statistics. However, no question exists whether the proportion of SNe Ib/c with $R \leqslant 2$ significantly exceeds the probability of chance superposition, making it very likely that the apparent associations for SNe Ib/c are indeed real. For the SNe II, we readily see that the proportions of apparent association greatly exceed the probability of chance superposition, and we confidently infer that the apparent associations found for SNe II are also real.

4. DISCUSSION

Our results are consistent with those of Kennicutt (1984), who used integrated Hα+[N II] flux from SNe parent galaxies, and found that the rate of SNe II in galaxies was linearly proportional to this flux, while the rate of SNe I (the distinction between SNe Ia and SNe Ib/c could not be made in 1984) was much more weakly correlated. Our results indicate that SNe Ia are not very likely to be physically associated with H II regions in late type galaxies and are therefore not associated with a massive short-lived (age $\lesssim 10^7$ yr) stellar population. It is evident that SNe Ib/c and SNe II are physically associated with recent star formation regions, and this strongly implies that both types have massive stars as progenitors.

Our results, however, do not strictly rule out the association of SNe Ia with an intermediate-age ($\gtrsim$ few times 10^7 yr) population (Oemler & Tinsley 1979; Filippenko 1989; van den Bergh 1990b), although Maza & van den Bergh (1976) found that SNe Ia show no preference for the spiral arm regions of galaxies and Della Valle & Panagia (1991) found that SNe Ia in late type galaxies are likely to have a z scale height at least twice that of dust in the galactic disk. Furthermore, the general homogeneity in observed properties for SNe Ia is difficult to reconcile with a dichotomy or range in progenitor populations. If SNe Ia arise from a population in late type galaxies with ages between a few times 10^7 yr and a few times 10^9 yr, then homogeneity would argue for a similar population of stars in elliptical and S0 galaxies, where it is generally thought that star formation has not likely occurred during this time interval. In a future paper we will consider the possible association of SNe with an intermediate-age population and the relationship of SNe Ia to the structure of the B-band light (which traces populations with ages $\lesssim 2 \times 10^9$ yr; Searle *et al.* 1973; Gallagher *et al.* 1984; Young *et al.* 1985) in the disks of late type galaxies. We suggest that the environments of SNe Ia in early type galaxies should also be investigated.

The proportion we find of SNe Ib/c with $R \leqslant 1$ is consistent with the results of Panagia & Laidler (1989), who found that $\sim$50%–60% of the SNe Ib/c appear to fall within $\sim 5''$ of a "knot" in the parent galaxies, which they presumed to be a H II region. However, Panagia & Laidler infer that SNe Ib/c are more loosely associated with H II regions than are SNe II, which would imply that the progenitors of SNe Ib/c are typically less massive than those of SNe II. For the small number of SNe Ib/c in our sample, we do not find that the proportion of SNe Ib/c associated with H II regions is significantly different from the proportion of SNe II associated with H II regions, and we therefore cannot make this same inference.

Our results for the SNe Ib/c do not support the single Wolf–Rayet star progenitor model. It is generally thought that these stars arise from precursors with zero-age main-sequence mass $\mathcal{M}_{\rm ZAMS} \gtrsim 30\,\mathcal{M}_\odot$, which is greater than the progenitor mass expected for SNe II (e.g., Woosley & Weaver 1986). Furthermore, these stars are strongly clustered near the cores of giant H II regions (e.g., d'Odorico *et al.* 1983; Melnick 1985; Moffat *et al.* 1987). If this model were correct, then the proportion of SNe Ib/c associated with H II regions should be substantially *greater* than that for SNe II, and this is clearly not the case (although we must still remain cautious of effects due to small-number statistics). It appears from our results that some other progenitor model, possibly an interacting binary system or even a single massive star (with mass similar to what is expected for SNe II progenitors), is more likely for SNe Ib/c. More data for the SNe Ib/c are clearly required.

Although we would not expect 100% correlations in any statistical study, it is interesting to consider the proportions of SNe Ib/c and SNe II *not* found to be associated with detected H II regions. It is possible that these proportions result from errors in the classifications and positions of some SNe. Gross errors in the published positions of early SNe II (SN 1921B, SN 1926A, and SN 1937F) could certainly account for their nonassociation. It is also possible that some nonassociated SNe II are misclassified, since two examples (SN 1937F and SN 1975T) were not spectroscopically classified, but were classified only on the basis of photometric light curves.

It is also possible that the progenitors of some nonassociated SNe II were "runaway" O stars, or star systems, since runaways may constitute as much as 46% of all Galactic O stars, with space velocities $\gtrsim 30$ km s^{-1} (Stone 1991). However, since velocity dispersions of unbound OB associations are generally too small (~ 10 km s^{-1}), SNe exploding in close O star binary systems (Stone 1991) or close star–star interactions in OB association cores (Gies 1985; Gies & Bolton 1986) are needed to catapult these stars. If it is a runaway with velocity $v \gtrsim 30$ km s^{-1}, a 9 $\mathcal{M}_\odot$ star with a lifetime of $\sim 3.3 \times 10^7$ yr (e.g., Maeder & Meynet 1988) will drift $\gtrsim 1$ kpc from its birthplace, while a 25 $\mathcal{M}_\odot$ star with lifetime $\sim 8.3 \times 10^6$ yr will drift $\gtrsim 300$ pc. Using galactic distances from Tully (1988), our results for R are not inconsistent with a runaway star hypothesis.

Furthermore, it is possible that some of these nonassociated SNe may have occurred in H II regions below our detection limit of $L_{\rm H\alpha} \sim 5 \times 10^{37}$ ergs s^{-1}. (This is not unreasonable, since van den Bergh & Tammann 1991 suggest that SNe should, in fact, be easier to discover in faint H II regions than in bright ones, unless they happen to be obscured by dense dust clouds.) Supporting this possibility is the appearance of "knots" of emission in the parent galaxies evident through broadband filters, but not detectable through the narrowband Hα filters. Examination of B-band images for the parent galaxies of four SNe II (SN

1941C, SN 1964A, SN 1980K, and SN 1985L) reveals that these SNe are apparently associated with small faint blue knots (presumably OB associations) along spiral arms in these galaxies. SN 1975T in NGC 3756 appears to have occurred along a faint extension of a spiral arm. The site of SN 1980K, which is $\sim 1'$ from a detected H II region, appears to be near a very faint knot seen on both a *B*-band and an *R*-band image of NGC 6946. Buta (1982) has pointed out that a faint object (with $B \geqslant 21$) was seen near the site of SN 1980K on a long-exposure photograph taken years prior to outburst.

In the case of SNe Ib/c not found associated with detected H II regions, the site of SN 1954A appears to be coincident with a dense, bright knot on an *R*-band image of its parent galaxy NGC 4214. However, no such "knot" was found at or near the site of SN 1966J in NGC 3198 from examination of both an *R*-band and a *B*-band image, although the SN appears to have occurred along the edge and toward the end of a spiral arm in that galaxy.

If the progenitors of SNe II also exist in low-luminosity H II regions, then they are not necessarily of lower mass than the progenitors of SNe II occurring in more luminous regions. Hunter & Massey (1990) found for the Galaxy that the stellar mass range extends up to fairly massive stars ($\mathcal{M} \sim 60\ \mathcal{M}_\odot$) even in H II regions with luminosities $\lesssim 10^{36}$ ergs s^{-1}. Possible association with low-luminosity H II regions, however, makes it unlikely that SNe II only arise from very massive stars with $\mathcal{M}_{\rm ZAMS} \sim 50$–$80\ \mathcal{M}_\odot$, as suggested by Richter & Rosa (1984), since such very massive stars are still quite rare in these regions. Interestingly, ~ 20 SNe II have occurred in Sa and Sb galaxies in which giant, luminous H II regions are relatively small in number, and in which the majority of massive star formation is occurring in fainter undetected H II regions (Kennicutt *et al.* 1989; Caldwell *et al.* 1991).

Finally, we can investigate any differences between the purported type II subclasses, SNe II-L and SNe II-P (Barbon *et al.* 1979). It is arguable whether an observational distinction actually exists between them. As van den Bergh (1988) points out, the distinctions between SNe II-L and SNe II-P were originally based on photographic, not strictly photoelectric, light curves, making any interpretations of the light curves imprecise. Younger & van den Bergh (1985) have found that SNe II comprise a photometrically nonhomogeneous group with a broad range of differences and no distinct subtypes. Nonetheless, Barbon *et al.* (1982) have argued that SNe II-L appear systematically brighter than SNe II-P and have distinguishable light curves. If a difference does exist, then it may be evident in the degree to which SNe II-L and SNe II-P are associated with H II regions, indicating differences between progenitors (van den Bergh 1988). If we make a distinction between SNe II-L and SNe II-P in Table 6, only three of seven SNe II-P have $R \leqslant 2$ and are associated with H II regions, while six of seven SNe II-L are. It is tempting to suggest that SNe II-L therefore may have more massive progenitors than do SNe II-P, but with so few objects, such a conclusion, like the actual subtype distinction itself, is probably unjustified.

Since we cannot clearly distinguish between the progenitors of SNe II and SNe Ib/c (at least from the statistics of their association with H II regions), since "transforming" SNe such as SN 1987K, which had the spectrum of a SN II in youth and of a SN Ib/c at later times, exist (Filippenko 1988b, 1991b), and since SNe such as SN 1991A possess characteristics of both types (Filippenko 1991a, 1992), it may be that the progenitors for both SNe Ib/c and SNe II are quite similar in mass. As van den Bergh (1988) has pointed out, the differences between SNe Ib/c and SNe II may only be "skin deep." Filippenko (1988a, 1988b, 1991b) has also recently alluded to a continuum in observed properties between the two classes and within each class. Differences in observed properties may arise from differences in envelope mass, core physics, density gradients in the envelope, binary evolution, mass loss, and convective mixing within the precursor stars, but all may originate from massive stars within a fairly narrow mass range. Our ability to understand such subtle differences appears to be just now emerging.

5. CONCLUSIONS

Our study of the association of SNe of types Ia, Ib/c, and II with regions of recent star formation, specifically giant H II regions, in late type galaxies yields the following results:

(1) It is unlikely that SNe Ia are associated with young massive stellar populations (with $\mathcal{M} \gtrsim 8\ \mathcal{M}_\odot$).

(2) Both SNe Ib/c and SNe II are likely to be associated with massive stellar populations.

(3) It is not evident whether the degree of association of SNe Ib/c and SNe II with H II regions are significantly different, although this result is subject to the effects of small-number statistics for SNe Ib/c. The single Wolf–Rayet star model for SNe Ib/c progenitors is not supported by our results. It is more likely that the interacting massive binary or other model is more appropriate. It is also possible that the progenitors of both types of SNe are actually very similar in mass range.

(4) The SNe Ib/c and SNe II not found to be associated with detected H II regions may have had runaway stars as progenitors or may have occurred in H II regions below our detection limit.

This paper was adapted from a Ph. D. dissertation done at the University of Washington (UW). Much gratitude is owed to Paul Hodge for his supervision of this work. Gratitude is also extended to George Wallerstein, Erika Böhm-Vitense, Karl-Heinz Böhm, Bruce Balick, Sidney van den Bergh, Kurt Weiler, and Ralph Fiedler for their input and comments during the course of this work. I am also grateful to Michael Rupen for his communications regarding SNe positions and for providing some finding charts, and to Rob Kennicutt, Bill Keel, and Jeff Kenney for providing some plates and CCD images. I gratefully acknowledge use of the 1.1 m telescope and the computing facilities of the Lowell Observatory. I also gratefully acknowledge assistance from the UW Department of Astronomy, the Na-

tional Optical Astronomy Observatories, the Department of Physics at Oklahoma State University, the Department of Physics & Astronomy at the University of Montana, the Center for Advanced Space Sensing at the Naval Research Laboratory, and the National Research Council. Finally, I thank an anonymous referee for helpful comments.

REFERENCES

Arsenault, R., & Roy, J.-R. 1986, AJ, 92, 567
Barbon, R., & Capaccioli, M. 1976, A&A, 49, 125
Barbon, R., Ciatti, F., & Rosino, L. 1973a, A&A, 29, 57
Barbon, R., Ciatti, F., & Rosino, L. 1973b, MSAIt, 44, 65
Barbon, R., Ciatti, F., & Rosino, L. 1979, A&A, 72, 287
Barbon, R., Ciatti, F., & Rosino, L. 1982, A&A, 116, 35
Barbon, R., Cappellaro, E., & Turatto, M. 1989, A&AS, 81, 421
Begelman, M. C., & Sarazin, C. L. 1986, ApJ, 302, L59
Bertaud, Ch. 1949, L'Astronomie 63, 65
Bertola, F. 1963, Contr. Asiago No. 135
Bertola, F. 1964, AJ, 69, 236
Bertola, F., & Ciatti, F. 1971, MSAIt, 42, 67
Bertola, F., Mammano, A., & Perinotto, M. 1965, Contr. Asiago No. 174
Boeshaar, G., & Hodge, P. W. 1977, ApJ, 213, 361
Branch, D. 1986, ApJ, 300, L51
Branch, D., & Nomoto, K. 1986, A&A, 164, L13
Burstein, D., & Heiles, C. 1984, ApJS, 54, 33
Buta, R. 1982, PASP, 94, 578
Caldwell, N., Kennicutt, R., Phillips, A. C., & Schommer, R. A. 1991, ApJ, 370, 526
Cappellaro, E., & Turatto, M. 1988, A&A, 190, 10
Ciatti, F., & Barbon, R. 1971, MSAIt, 42, 145
Ciatti, P., & Rosino L. 1977, A&A, 57, 73
Courtes, G. 1977, in Topics in Interstellar Matter, edited by H. van Woerden (Reidel, Dordrecht), p. 209
Curtis, H. D. 1917, PASP, 29, 180
de Goioa-Eastwood, K., Grasdalen, G. L., Strom, S. E., & Strom, K. M. 1984, ApJ, 278, 564
Della Valle, M., & Panagia, N. 1991, ApJ, in press
Detre, L. 1969, IAU Circ., No. 2134
de Vaucouleurs, G., de Vaucouleurs, A., & Corwin, Jr., H. G. 1976, Second Reference Catalog of Galaxies (University of Texas Press, Austin)
d'Odorico, S., Rosa, M., & Wampler, E. J. 1983, A&AS, 53, 97
Doggett, J. B., & Branch, D. 1985, AJ, 90, 2303
Dufour, R. J. 1975, ApJ, 195, 315
Dunlap, J. R. 1971a, IAU Circ., No. 2330
Dunlap, J. R. 1971b, IAU Circ., No. 2336
Ensman, L. M., & Woosley, S. E. 1988, ApJ, 333, 754
Evans, R. van den Bergh, S., & McClure, R. D. 1989, ApJ, 345, 752
Filippenko, A. V. 1988a, IAU Circ., No. 4597
Filippenko, A. V. 1988b, AJ, 96, 1941
Filippenko, A. V. 1989, PASP, 101, 588
Filippenko, A. V. 1990, IAU Circ., No. 4953
Filippenko, A. V. 1991a, IAU Circ., No. 5169
Filippenko, A. V. 1991b, in SN 1987A and Other Supernovae, edited by I. J. Danziger and K. Kjär (ESO, Garching bei München), p. 343
Filippenko, A. V. 1992, ApJ, 384, L37
Filippenko, A. V., & Sargent, W. L. W. 1985, Nature, 316, 407
Filippenko, A. V., & Sargent, W. L. W. 1986, AJ, 91, 691
Filippenko, A. V., & Shields, J. C. 1990, IAU Circ., No. 5111
Flin, P., Karpowicz, M., Murawski, W., & Rudnicki, K. 1979, Acta Cosmologica No. 8 (Jagellonian University Observatory, Poland)
Fransson, C., & Chevalier, R. A. 1989, ApJ, 343, 323
Gallagher, J. S., Hunter, D., & Tutukov, A. V. 1984, ApJ, 284, 544
Gaskell, C. M., Cappellaro, E., Dinerstein, H., Garnett, D., Harkness, R. P., & Wheeler, J. C. 1986, ApJ, 306, L77
Gates, H. S., Zwicky, F., Bertola, R., Ciatti, F., & Rudnicki, K. 1967, AJ, 72, 912, 927
Gies, D. R. 1985, Ph. D. thesis, University of Toronto
Gies, D. R., & Bolton, C. T. 1986, ApJS, 61, 419
Gunn, J. E., & Stryker, L. 1983, ApJS, 52, 121
Hachisu, I., Matsuda, T., Nomoto, K., & Shigeyama, T. 1991, ApJ, 368, L27
Harkness, R. P., & Wheeler, J. C. 1990, in Supernovae, edited by A. G. Petschek (Springer, New York), p. 1
Harkness, R. P., Wheeler, J. C., Margon, B., Downes, R. A., Kirshner, R. P., Uomoto, A., Barker, E. S., Cochran, A. L., Dinerstein, H. L., Garnett, D. R., & Levreault, R. M. 1988, ApJ, 317, 355
Haro, G. 1965, IAU Circ., No. 1908
Hodge, P. W. 1966, Atlas and Catalogue of H II Regions (University of Washington, Seattle)
Hodge, P. W. 1969, ApJS, 18, 73
Hodge, P. W. 1974, ApJS, 27, 113
Hodge, P. W. 1982, AJ, 87, 1341
Hodge, P. W. 1986, private communication
Hodge, P. W., & Kennicutt, Jr., R. C. 1983, Atlas of H II Regions in 125 Galaxies (University of Washington, Seattle)
Huang, Y.-L. 1987, PASP, 99, 461
Hubble, E., & Moore, G. 1936, PASP, 48, 108
Humason, M. L., Gomes, A. M., & Kearns, C. E. 1961, PASP, 73, 175
Hunter, D. A., & Massey, P. 1990, AJ, 99, 846
Jacoby, G. H., Hunter, D. A., & Christian, C. A. 1984, ApJS, 56, 257
Jones, R. 1941a, Harvard Ann. Card No. 576
Jones, R. 1941b, IAU Circ., No. 866
Keel, W. C. 1983, ApJS, 52, 229
Keel, W. C. 1989, private communication
Keel, W. C., Kennicutt, Jr., R. C., Hummel, E., & van der Hulst, J. M. 1985, AJ, 90, 708
Kenney, J. D. 1990, private communication
Kennicutt, Jr., R. C. 1978, Ph. D. thesis, University of Washington
Kennicutt, Jr., R. C. 1984, ApJ, 277, 361
Kennicutt, Jr., R. C. 1986, private communication
Kennicutt, Jr., R. C. 1988, ApJ, 334, 144
Kennicutt, Jr., R. C. 1991, in Massive Stars in Starbursts, edited by C. Leitherer, N. R. Walborn, T. M. Heckman, and C. A. Norman (Cambridge University Press, Cambridge), p. 157
Kennicutt, Jr., R. C., Edgar, B. K., & Hodge, P. W. 1989, ApJ, 337, 761
Kirshner, R. P. 1990, in Supernovae, edited by A. G. Petschek (Springer, New York), p. 59
Kirshner, R., & Leibundgut, B. 1990, IAU Circ., No. 4953
Koornneef, J. 1978, A&A, 64, 179
Kowal, C. T., Zwicky, F., Sargent, W. L. W., & Searle, L. 1974, PASP, 86, 516
Leibundgut, B. 1991, BAAS, 23, 882
Leibundgut, B., & Tammann, G. A. 1990, A&A, 230, 81
Löchel, K. 1965, Info. Bull. Var. Stars No. 113
Maeder, A., & Meynet, G. 1988, A&AS, 76, 411
Marsden, B. G. 1982, IAU Circ., No. 3746
Mayall, N. U. 1948, Harvard Ann. Card No. 912
Maza, J., & van den Bergh, S. 1976, ApJ, 204, 519
Melnick, J. 1985, A&A, 153, 235
Moffat, A. F. J., Niemela, V. S., Phillips, M. M., Chu, Y. H., & Seggewiss, W. 1987, ApJ, 312, 612
Moore, C. E., Minnaert, M. G. J., & Houtgast, J. 1966, Solar Spectrum 2935 Å to 8770 Å, NBS Monograph No. 61
Muller, R. A., Newberg, H. J. M., Pennypacker, C. R., Perlmutter, S., Sasseen, T. P., & Smith, C. K. 1992, ApJ, 384, L9
Nomoto, K. 1986, in Origin and Evolution of Neutron Stars, edited by D. J. Helfand and J. H. Huang (Reidel, Dordrecht)
Nomoto, K., Filippenko, A. V., & Shigeyama, T. 1990, A&A, 240, L1
Odewahn, S. C. 1991a, AJ, 101, 829
Odewahn, S. C. 1991b, private communication
Oemler, A., & Tinsley, B. M. 1979, AJ, 84, 985

Palumbo, G. G. C., Tanzella-Nitti, G., & Vettolani, G. 1983, Catalog of Radial Velocities of Galaxies (Gordon and Breach, New York)
Panagia, N., & Laidler, V. G. 1989, in Supernova Shells and their Birth Events, edited by W. Kundt (Springer, Berlin), p. 187
Patchett, B., & Wood, R. 1976, MNRAS, 175, 595
Pennypacker, C. 1987, IAU Circ., No. 4426
Pennypacker, C., Burns, S., Crawford, F., Friedman, P., Muller, J., Perlmutter, S., Smith, C., Treffers, R., Williamson, A., & Junkkarinen, V. 1986, IAU Circ., No. 4219
Perlmutter, S., & Pennypacker, C. 1988, IAU Circ., No. 4590
Perlmutter, S., & Pennypacker, C. 1990, IAU Circ., No. 4949
Piembert, M., & Torres-Piembert, S. 1974, ApJ, 193, 327
Piembert, M., & Torres-Piembert, S. 1976, ApJ, 203, 581
Porter, A. C. 1987, IAU Circ., No. 4470
Richter, O.-G., & Rosa, M. 1984, A&A, 140, L1
Rosino, L. 1964, IAU Circ., No. 1873
Rosino, L. 1969, IAU Circ., No. 2134
Rupen, M. P. 1991, private communication
Sandage, A., & Tammann, G. 1981, A Revised Shapley-Ames Catalog of Bright Galaxies (Carnegie, Washington, DC)
Schlegel, E. 1990, MNRAS, 244, 269
Schürer, M. 1966, IAU Circ., No. 1986
Schürer, M. 1974, IAU Circ., No. 2664
Searle, L. 1976, IAU Circ., No. 2984
Searle, L., Sargent, W. L. W., & Bagnuolo, W. 1973, ApJ, 179, 427
Shapley, H. 1939, Proc. Nat. Ac. Sci., 25, 569
Shigeyama, T., Nomoto, K., Tsujimoto, T., & Hashimoto, M. 1990, ApJ, 361, L23
Sinclair, J. E. 1985, IAU Circ., No. 4084
Stone, R. C. 1991, AJ, 102, 333
Swartz, D. A., & Wheeler, J. C. 1991, ApJ, 379, L13
Tammann, G. A. 1982, in Supernovae: A Survey of Current Research, edited by M. J. Rees & R. J. Stoneham (Reidel, Dordrecht), p. 371
Tammann, G. A., & Leibundgut, B. 1990, A&A, 236, 9
Thompson, L. A. 1982, ApJ, 257, L63
Tsvetkov, D. Yu. 1985, SvAJ, 29, 211
Tully, R. B. 1974, ApJS, 27, 437
Tully, R. B. 1988, Nearby Galaxies Catalog, Cambridge (Cambridge University Press, Cambridge)
Uomoto, A. K. 1986, ApJ, 310, L35
van den Bergh, S. 1988, ApJ, 327, 156
van den Bergh, S. 1990a, A&A, 231, L27
van den Bergh, S. 1990b, PASP, 102, 1318
van den Bergh, S., & McClure, R. D. 1990, ApJ, 359, 277
van den Bergh, S., & Tammann, G. A. 1991, ARA&A, 29, 363
Viallefond, F., & Goss, W. M. 1986, A&A, 154, 357
Weiler, K. W., Sramek, R. A., & Panagia, N., van der Hulst, J. M., & Salvati, M. 1986, ApJ, 301, 790
Weiler, K. W., Van Dyk, S. D., Panagia, N., Sramek, R. A., & Discenna, J. L. 1991, ApJ, 380, 161
Wheeler, J. C. 1985, IAU Circ., No. 4053
Wheeler, J. C., & Harkness, R. P. 1990, Rept. Progr. Phys., 53, 1467
Wild, P. 1954, Harvard Ann. Card No. 1250
Wild, P. 1960, PASP, 72, 97
Wild, P. 1961, IAU Circ., No. 1753
Wild, P. 1968, IAU Circ., No. 2057
Wild, P. 1972, IAU Circ., No. 2476
Wild, P. 1975, IAU Circ., No. 2895
Wild, P. 1978, IAU Circ., No. 3303
Woosley, S. E., & Weaver, T. A. 1986, ARA&A, 24, 205
Young, J. S., Scoville, N. Z., & Brady, E. 1985, ApJ, 288, 487
Younger, P. F., & van den Bergh, S. 1985, A&AS, 61, 365
Zwicky, F. 1964, Ann. Ap. 27, 300
Zwicky, F. 1965, Stars and Stellar Systems, Vol. VIII, edited by L. H. Aller and D. B. McLaughlin (University of Chicago Press, Chicago), p. 367
Zwicky, F. 1967, IAU Circ., No. 2021
Zwicky, F. 1968, PASP, 80, 462
Zwicky, F., & Karpowicz, M. 1965, AJ, 69, 759